October 1998 • NREL/SR-520-25613

Alternative Window Schemes for $CuInSe_2$-Based Solar Cells

Final Report
3 November 1995—December 1997

L.C. Olsen
Electronic Materials Laboratory
Washington State University at Tri-Cities
Richland, Washington

National Renewable Energy Laboratory
1617 Cole Boulevard
Golden, Colorado 80401-3393
A national laboratory of the U.S. Department of Energy
Managed by Midwest Research Institute
for the U.S. Department of Energy
under contract No. DE-AC36-83CH10093

NREL/SR-520-25613

Alternative Window Schemes for $CuInSe_2$-Based Solar Cells

Final Report
3 November 1995—December 1997

L.C. Olsen
Electronic Materials Laboratory
Washington State University at Tri-Cities
Richland, Washington

NREL technical monitor: B. von Roedern

National Renewable Energy Laboratory
1617 Cole Boulevard
Golden, Colorado 80401-3393
A national laboratory of the U.S. Department of Energy
Managed by Midwest Research Institute
for the U.S. Department of Energy
under contract No. DE-AC36-83CH10093

Prepared under Subcontract No. XAF-6-15375-01

October 1998

This publication was reproduced from the best available copy
Submitted by the subcontractor and received no editorial review at NREL

NOTICE

This report was prepared as an account of work sponsored by an agency of the United States government. Neither the United States government nor any agency thereof, nor any of their employees, makes any warranty, express or implied, or assumes any legal liability or responsibility for the accuracy, completeness, or usefulness of any information, apparatus, product, or process disclosed, or represents that its use would not infringe privately owned rights. Reference herein to any specific commercial product, process, or service by trade name, trademark, manufacturer, or otherwise does not necessarily constitute or imply its endorsement, recommendation, or favoring by the United States government or any agency thereof. The views and opinions of authors expressed herein do not necessarily state or reflect those of the United States government or any agency thereof.

Available to DOE and DOE contractors from:
Office of Scientific and Technical Information (OSTI)
P.O. Box 62
Oak Ridge, TN 37831
Prices available by calling (423) 576-8401

Available to the public from:
National Technical Information Service (NTIS)
U.S. Department of Commerce
5285 Port Royal Road
Springfield, VA 22161
(703) 605-6000 or (800) 553-6847
or
DOE Information Bridge
http://www.doe.gov/bridge/home.html

Printed on paper containing at least 50% wastepaper, including 10% postconsumer waste

TABLE OF CONTENTS

ABSTRACT i

1. INTRODUCTION 1

    1.1 Background 1
    1.2 Program Objectives 2
    1.3 Technical Approach 2

2. ZnO BUFFER STUDIES 4

    2.1 MOCVD Growth Of ZnO 4
    2.2 ZnO Layer Optimization 4
    2.3 Physical Characterization Of ZnO Buffer Layers 9
    2.4 Solar Cell Studies 12

3. ZnSe BUFFER LAYER STUDIES 16

4. In_xSe_y BUFFER LAYER STUDIES 18

5. SIMULATION STUDIES 20

6. CONCLUSIONS 22

ACKNOWLEDGMENTS 23

REFERENCES 23

ABSTRACT

This work has resulted in the demonstration of high efficiency CIGS cells based on highly resistive ZnO buffer layers grown by MOCVD. One cell based on NREL CIGS and a ZnO buffer layer exhibited an active area efficiency of nearly 14 %. This result is one of the best efficiencies reported for a "direct" ZnO/CIGS cell made with a vacuum process. This work has established that the buffer layer is truly ZnO, and not an alloy resulting from interdiffusion of ZnO and CIGS. It has also been established that a two step growth procedure like those described as 'baseline' and 'modified' lead to efficient cells. In order to achieve high efficiencies, it is necessary for ZnO buffer layers to have resistivities greater than 10^4 ohm-cm. Efficient cells are obtained whether the high resistivity is achieved as-grown, or after exposure to air. Since cell efficiencies are lower than predicted by simulation studies when the buffer resistivity is lower than 10^4 ohm-cm, we conclude that the resistivity is simply related to processing. In particular, the resistivity correlates with the excess zinc in the MOCVD ZnO film, which can in turn diffuse into the CIS absorber and possibly cause enhanced current loss mechanisms. Future studies will focus on identifying process pathways that will lead to resistive ZnO buffer layers, and thus large cell efficiencies. A limited effort was devoted to ZnSe buffer layers. A completed cell with a ZnSe buffer layer and RF sputtered ZnO TCO was fabricated and produced power with a total area efficiency of 9.5 %. Future studies will concentrate on the development of approaches to deposit conductive ZnO on top of the ZnSe buffer layer without degrading properties of the ZnSe/CIS structure.

1. INTRODUCTION

This report concerns work carried out during the time period 11/03/95 through 12/31/97 to investigate alternative window layers (buffer layers) for solar cell structures based on CIS and CIS alloys. In particular, ZnSe, ZnO and InSe films were examined as potential, alternative (to CdS) window layers for CIS cells. Background information, program objectives and the technical approach are discussed in the remainder of this section, and technical progress made during the program is discussed in subsequent sections.

1.1 Background

The major objective of this program was to determine the potential of ZnSe and ZnO buffer layers in solar cells based on $CuInSe_2$ and related alloys. Experimental studies were carried out with CIS and CIGSS substrates provided by Siemens Solar. ZnSe films were deposited by a CVD process which involved the reaction of a zinc adduct and H_2Se. Al/ZnSe/CIS test cells were used for process development. Test cell performance aided in determining the optimum thickness for ZnSe buffer layers to be in the range of 150Å to 200Å for Siemens CIS material, and between 80Å and 120Å for the graded absorber material (CIGSS). If the buffer layers exceeded these values significantly, the short-circuit current would be reduced to zero. This effect is consistent with results reported in the literature indicating that there is a 0.9 eV band offset at the ZnSe-CIS interface. Completed cells were fabricated by utilizing a low resistance ZnO top contact layer deposited by Siemens, and then depositing an Al/Ag collector grid at WSU. The best efficiency achieved for a ZnSe/CIS cell was an active area value of 9.2 %. In general, deposition of a conductive ZnO film on top of a ZnSe/CIS structure resulted in either shunted or inflected I-V characteristics. Two approaches were investigated for depositing ZnO buffer layers, namely, chemical bath deposition and chemical vapor deposition. CVD ZnO buffer layers are grown by reacting a zinc adduct with tetrahydrofuran. Best results were obtained for ZnO buffer layers grown with a substrate temperature

(T_{sub}) ≈ 225°C to 250°C. These studies concentrated on Siemens graded absorber material (CIGSS). ZnO/CIS solar cells have been fabricated by first depositing a ZnO buffer layer, followed by deposition of a low resistivity ZnO top contact layer and an Al/Ag collector grid. Several cells were fabricated with an area of 0.44 cm^2 that have total area efficiencies greater than 11 %. To date, the best performing ZnO/CIS cell was measured by NREL to have a total area, AM1.5G efficiency of 11.3 %. The active area efficiency of the device was approximately 12 %, which appears to be the best result for a ZnO buffer layer. In general, we find that ZnO buffer layers should have a resistivity > 1000 ohm-cm and have a thickness from 200 Å to 600 Å. CIS cells studies with ZnO buffer layers grown by CBD also show promise. Finally, simulation studies were carried out using the one-dimensional code, PC-1D.

1.2 Program Objectives

The objectives of this program are: to develop alternate heterojunction partner layers for high efficiency $CuInSe_2$-based thin film solar cells; and, to improve the understanding regarding the effects of these buffer layers and related processing upon cell performance.

1.3 Technical Approach

The general approach to these studies has consisted of utilizing substrates provided by industry and NREL, so that efforts could focus on buffer layer investigations. MOCVD growth of buffer layers is accomplished with a SPIRE 500XT reactor with added gas handling capabilities. Optimum processing parameters for candidate buffer layers are determined by characterizing Al/X/CIS test cell structures, where X refers to a heterojunction partner. Semitransparent Al films with thicknesses in the range of 100 to 150 Å are utilized so that illuminated I-V characteristics can be obtained for the test structure. After the buffer-layer growth parameters are determined, completed solar cell structures are fabricated and evaluated. Layers and devices are characterized at WSU and with the help of

collaboration with NREL. Efforts this past year concentrated on studies of highly resistive ZnO buffer layers grown by MOCVD.

Substrates provided by Siemens and NREL consist of a CIS-based absorber layer grown on Mo-coated glass. The Siemens absorber is of the form $Cu(In,Ga)Se_2$ with the Ga concentrated at the back of the absorber structure[1]. Quantum efficiency data taken for this type of material exhibited an effective bandgap of 0.95 eV. Thus, the Siemens substrates are referred to as CIS substrates in this report. NREL absorber layers were grown with a 3-stage process that has been discussed previously [2]. These absorbers exhibit effective bandgaps in the range of 1.05 to 1.15 eV, and will therefore be referred to CIGS substrates. TCO deposition, contact formation and cell testing were carried out by NREL and IEC.

2. ZnO BUFFER LAYER STUDIES

2.1 MOCVD Growth Of ZnO

ZnO buffer layers are grown by metal organic chemical vapor deposition (MOCVD) by reacting a zinc adduct with tetrahydrofuran and utilizing hydrogen as a carrier gas. Prior to growth of buffer layers, substrates were subjected to a degreasing process consisting of rinses in TCA, acetone, methanol and DI water. Substrate temperatures (T_{sub}) have been varied from 100°C to 250°C. Further discussion of growth procedures is given below.

2.2 ZnO Layer Optimization

Optimization of processing parameters for ZnO buffer layers has been aided by fabrication and characterization of Al/ZnO/CIS test cells. After growing a ZnO film on a CIS substrate, an array of thin, optically transparent Al circular areas 2.8 mm in diameter are deposited onto the ZnO/CIS structure. Illuminated characteristics of test cells are measured by illuminating the device such that $J_{sc} \approx 40$ mA/cm^2 for Siemens CIS substrates (not containing sulfur) , and 36 mA/cm^2 for CIGS substrates. The cell efficiency determined using this procedure may be regarded as an estimated active area value, assuming that one can add a top contact layer and collector grid without degrading the junction properties. Although aluminum is quite reactive, these test cells provide useful information regarding Buffer layer properties since the ZnO films are typically $\geq$ 500 Å thick, which makes the ZnO-Al interface relatively far from the ZnO-CIS interface. Figure 1 shows results for test cell efficiency vs ZnO layer resistivity. The resistivity refers to a value determined for a film grown simultaneously on a glass witness and measured immediately after the growth run. The fill factor is particularly sensitive to the ZnO layer resistivity, with low values of fill factor occurring for low resistivities and larger fill factors resulting when the buffer layer resistivities are relatively large. The low efficiencies obtained for devices with relatively low resistivity ZnO layers are consistent with reported results for direct ZnO cells based on deposition of low resistivity n-ZnO

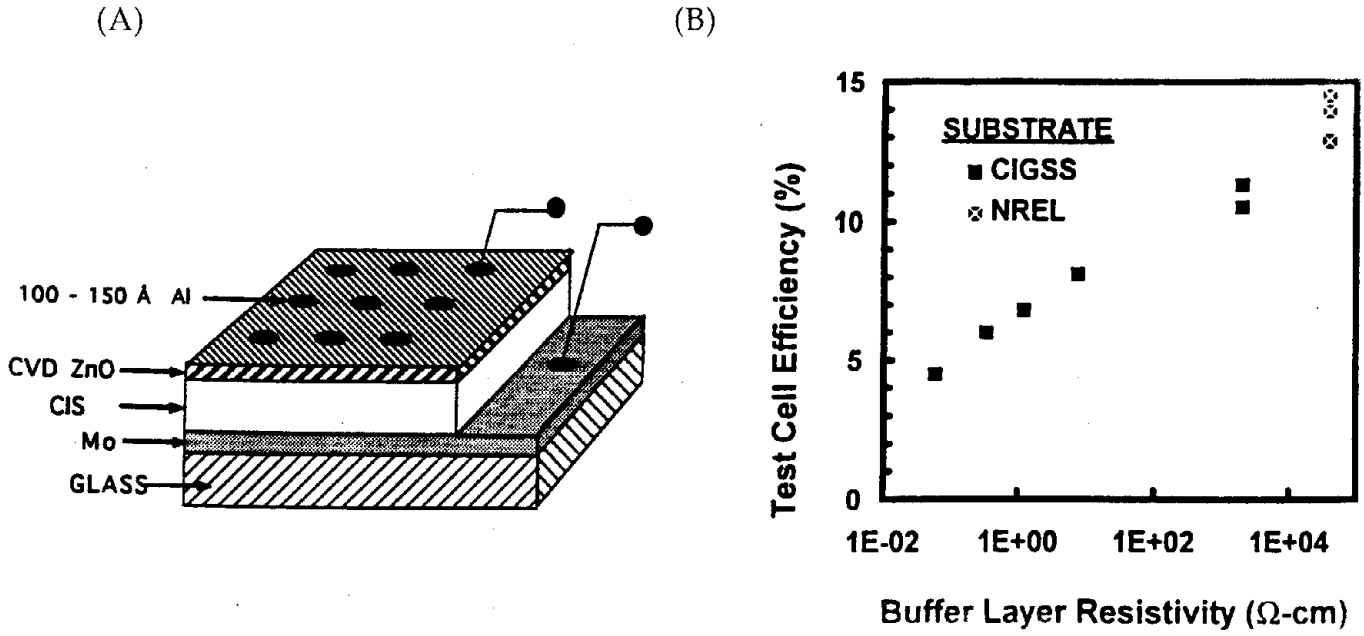

Figure 1. (A) Test Cell Configuration. (B) Test cell efficiency vs as-grown resistivity of CVD ZnO buffer layers.

directly onto CIS [4]. These studies indicated that the ZnO buffer layers should have high resistivities, namely, at least as high as ≈ 10,000 ohm-cm. It should be emphasized that we regard the resistivity simply as a process parameter.

Optimization studies have led to a two step process for growth of ZnO buffer layers. A run profile used for the two step process is described in Figure 2. The first step involves growth of approximately 100 Å of ZnO at 250°C, while the second step consists of depositing approximately 500 to 800 Å of ZnO at 100°C. This approach was originally motivated by the observation that films grown at 250°C exhibited slightly larger grain sizes and smoother morphologies than those grown at 100 °C. Investigations indicated that the time of growth at 250°C should be limited so that interdiffusion effects could be minimized. The two-step approach has been used to produce completed solar cells with high efficiencies. Studies are in progress to understand the significance of each step. Since the WSU process utilizes hydrogen as a carrier gas, one question being addressed concerns the potential positive effect of

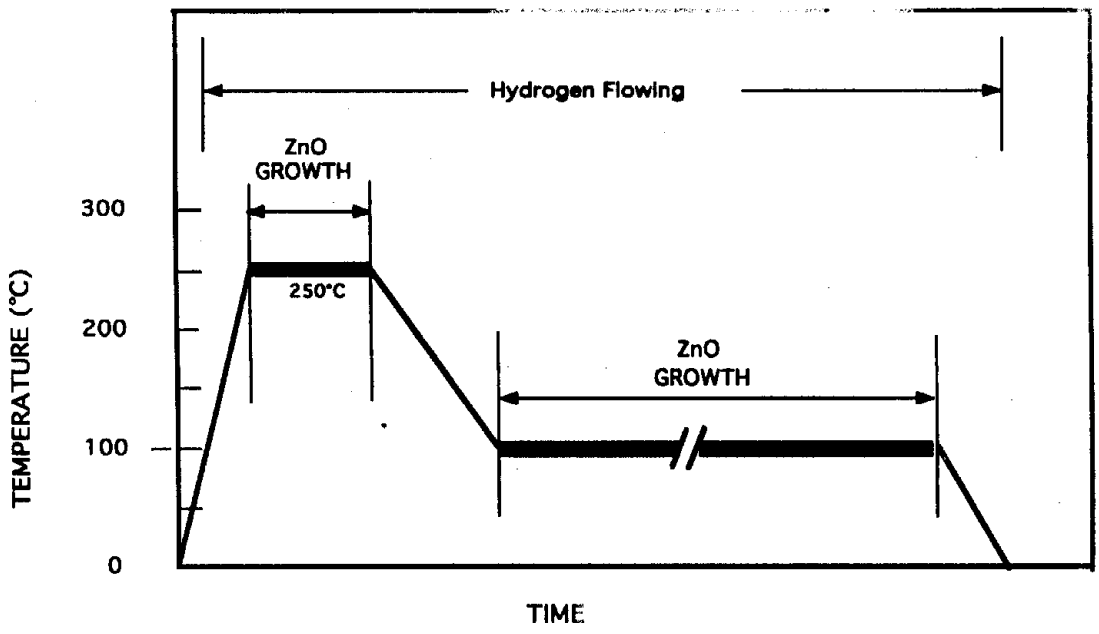

Figure 2. Growth run profile used for the two-step process for CVD ZnO.

hydrogen.

Process development has involved examination of variations of the two-step procedure described by Figure 2 (referred to as the baseline process). Figure 3 describes three processes including the baseline approach It was determined that the modified process leads to cells with nearly as good performance as achieved with the baseline process (see Figure 4). However, a single step process involving ZnO growth at 100°C gives very poor results, whereas the inclusion of a first step involving heating the sample to 250°C before growth of ZnO at 100°C leads to very good cell performance Based on results obtained to date, it appears that growth of ZnO during the first step may not be important.

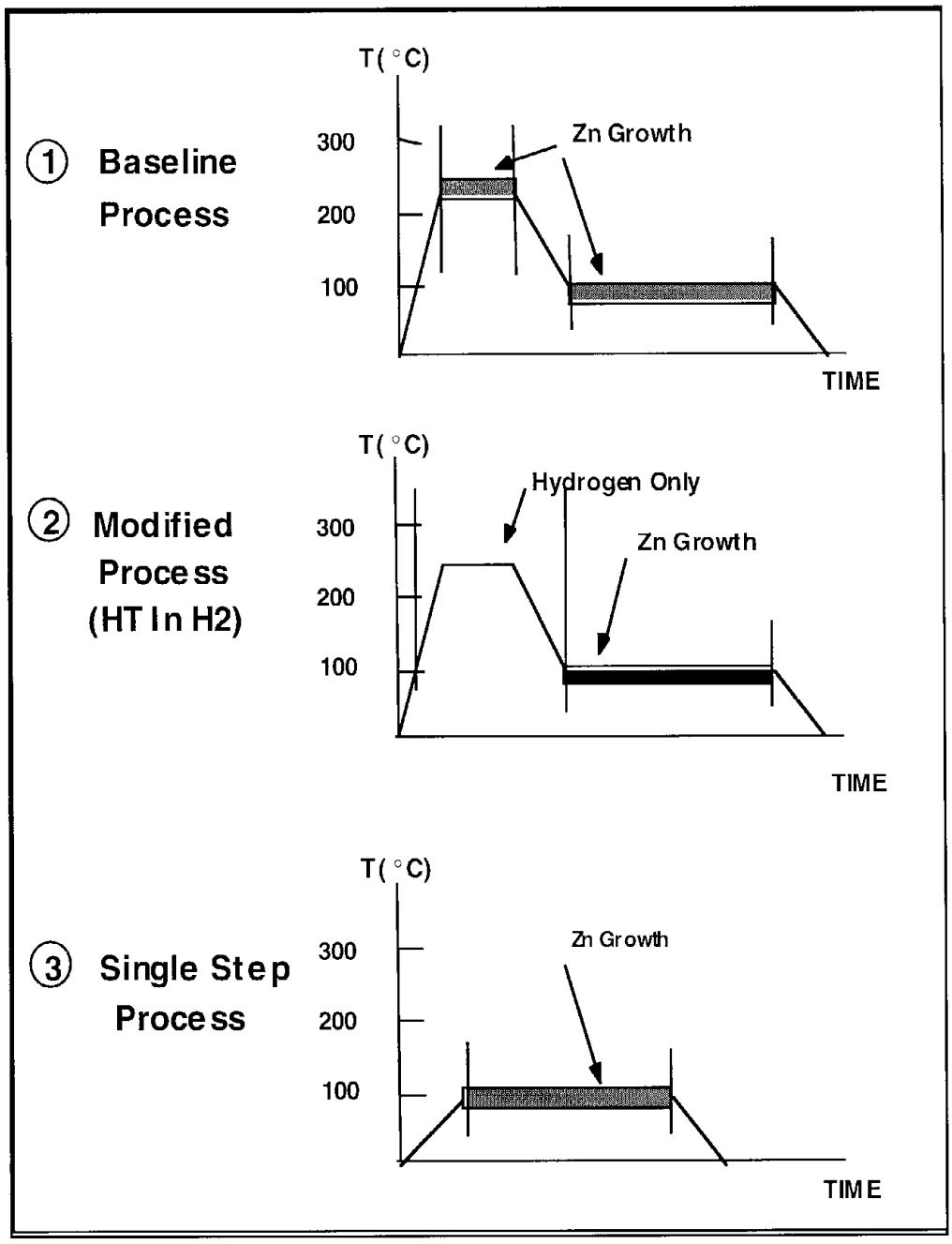

Figure 3. Three MOCVD growth schedules utilized for deposition of ZnO buffer layers.

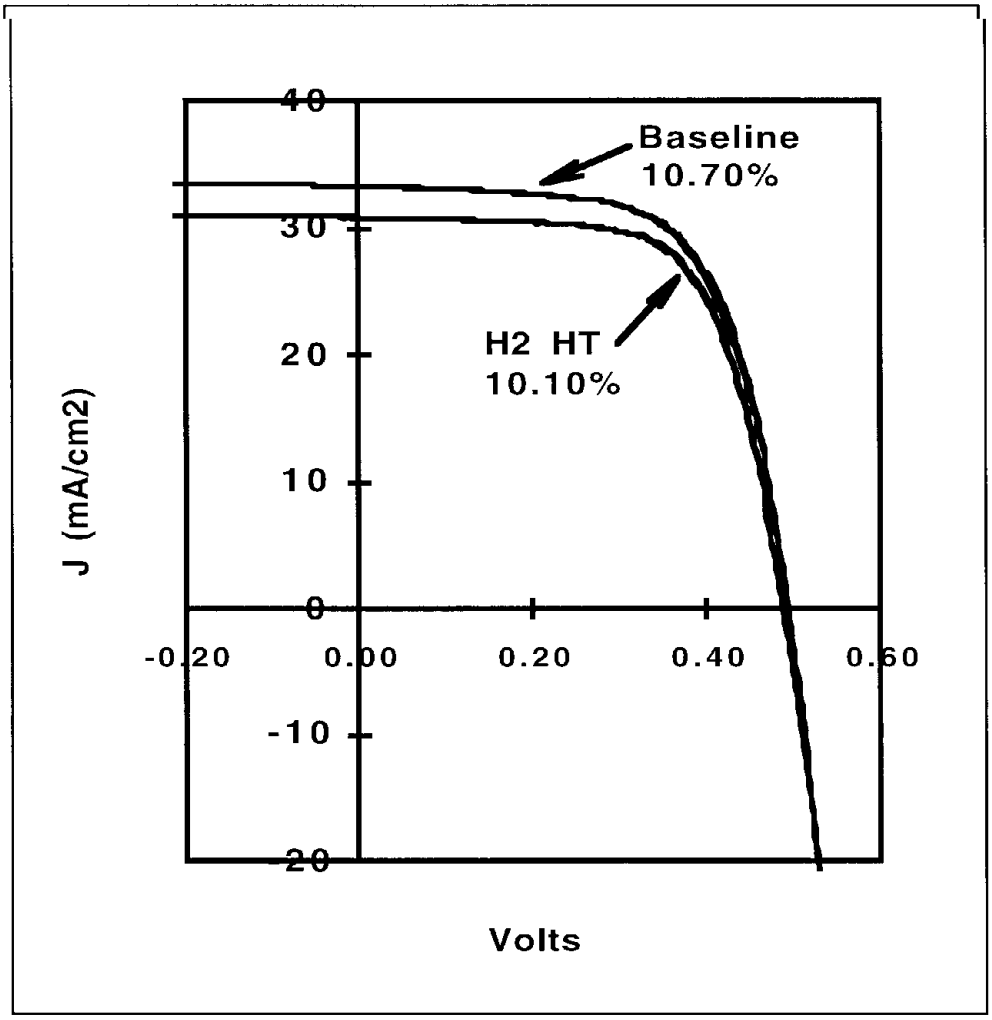

Figure 4. Total area illuminated I-V characteristics for cells with MOCVD ZnO buffer layers.

It is not yet clear whether the presence of hydrogen during the first step for both the baseline and modified processes is critical to achieving high efficiency CIGS cells with MOCVD ZnO buffer layers. Surface AES profiles taken on NREL CIGS absorbers indicate that CIGS sample surfaces are readily contaminated with oxygen and carbon after exposure to air. Even though substrates are cleaned prior to insertion into the MOCVD chamber for growth of ZnO, one would expect that the sample surfaces would acquire these contaminants. Thus, one effect of the 250°C step may simply be to cleanse the surface of contaminants. Additional experiments will be conducted to determine if the presence of hydrogen is important.

2.3 Physical Characterization Of ZnO Buffer Layers

ZnO films have been characterized with XPS, GIXRD and ellipsometry. The sample configuration used for the studies is described in Figure 5. XPS measurements were carried out with a Physical Electronics Quantum 2000 XPS system at the Pacific Northwest National Laboratory (PNNL). The XPS studies were conducted to determine the nature of film coverage and to identify any impurities in the ZnO films. Figure 6 gives results for XPS scans near In_{3d5} and In_{3d3} lines for three films grown as described in Figure 6A. The process for the first film was terminated at the end of the 250°C step, whereas the second and third films were grown by terminating the process (separate runs) at positions 2 and 3 as indicated. The ZnO film thicknesses in the three cases were approximately 100 Å, 200 Å and 800 Å. XPS data were acquired for each sample. No signals associated with Cu or Se were detected for any of the runs. However, In peaks were observed in cases No. 1 and No. 2. Two conclusions can be made. Apparently, good coverage is achieved after

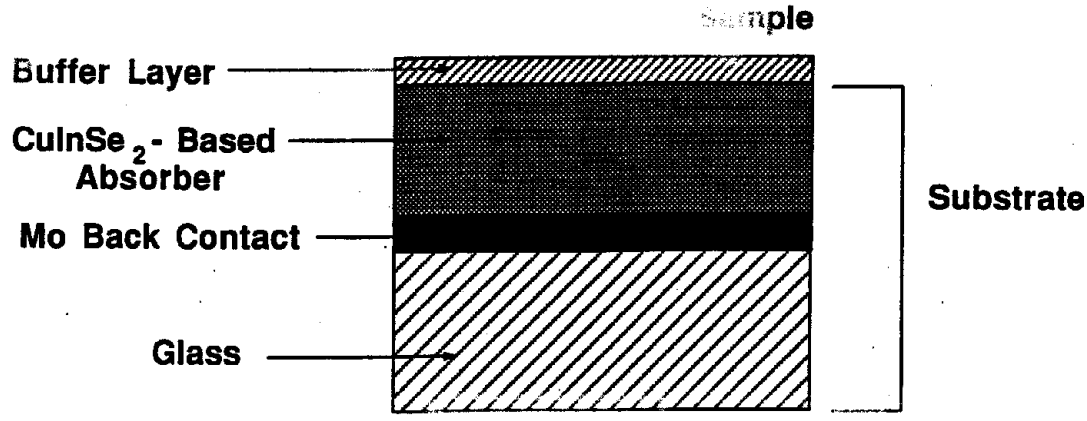

Figure 5. Description of CIS substrate and sample used for buffer layer characterization.

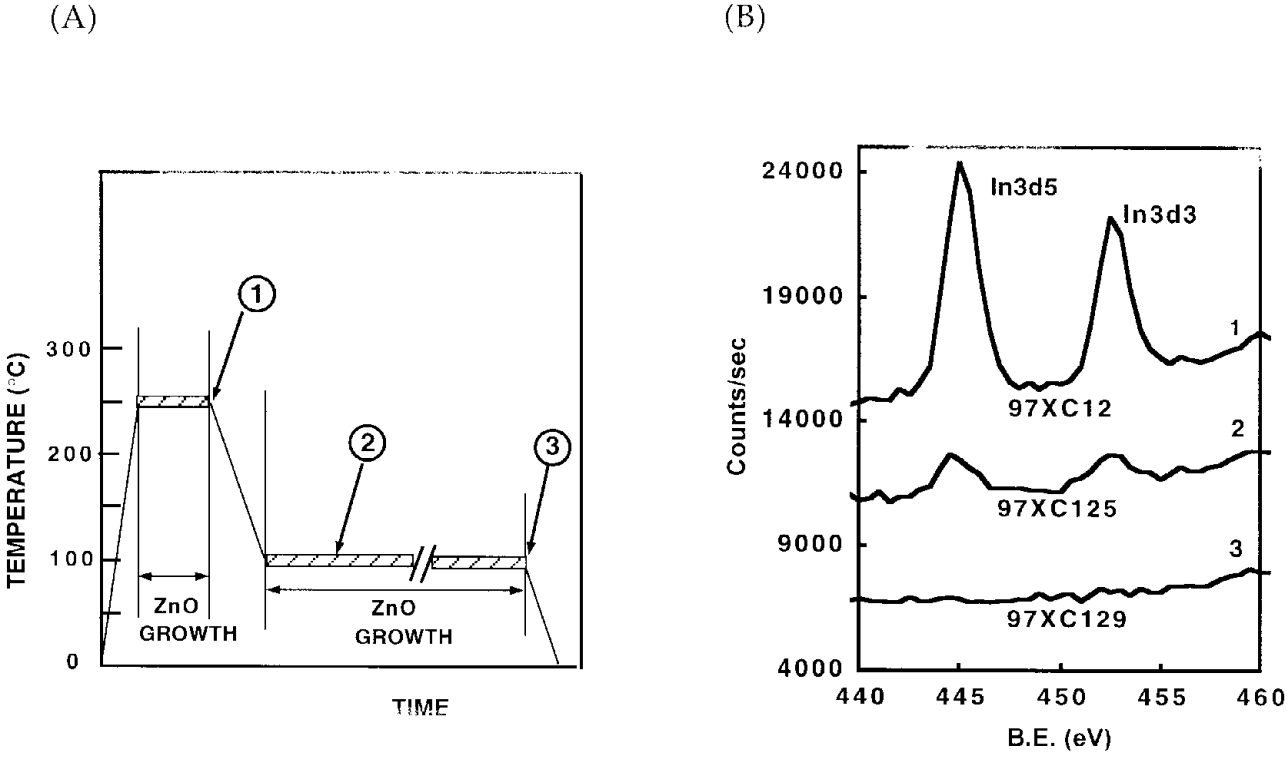

Figure 6. (A) Qualitative descriptive description of approach to MOCVD growth of ZnO buffer layers. The three points indicate where growth was terminated for XPS studies . (B) XPS results for three films for which growth was terminated at Positions 1, 2 and 3.

100 Å of growth (after Step 1) since no signals from Cu and Se are detected, but In apparently diffuses outward as the film grows. No In is detected at position 3 (on the surface of the 800 Å film), and is only weakly detected at position 2 (after ≈ 200 Å of ZnO growth). The In could be in the form of In_2O_3 or in substitutional positions in the ZnO lattice, which would result in increased conductivity.

Figure 7 shows an XPS survey scan taken on the sample corresponding to Position 3 indicates that the film is comprised of only Zn and oxygen. The strong Zn_{2p1}, Zn_{2p3}, Zn_{3p3} and Zn_{3s} peaks plus Zn Auger lines indicate a typical pattern for ZnO. Note that there is no signal due to Na. The O1s peak is shifted +2 eV compared to reports in the literature, indicating a higher O1s binding energy. This

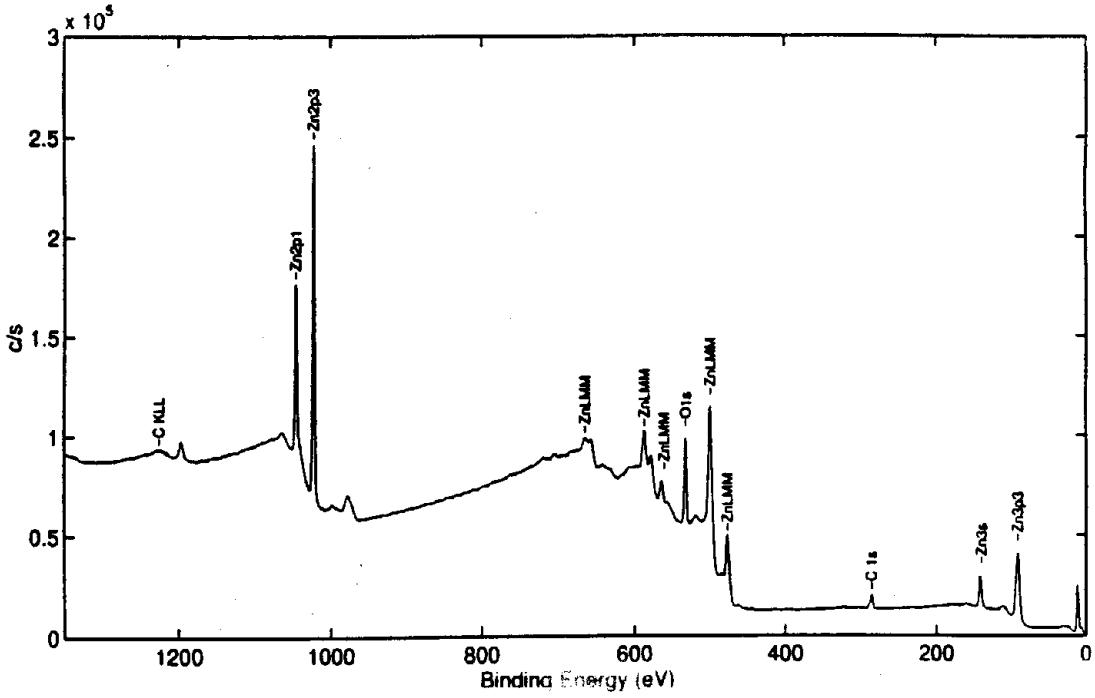

Figure 7. A wide XPS scan taken on the ZnO/CIS sample for which the ZnO growth was terminated at Point 3 (800 Å film).

result is consistent with the films being deficient in oxygen. GIXRD results discussed below also suggest that the MOCVD films were oxygen deficient.

GIXRD data taken at NREL revealed that the WSU ZnO films grown by CVD on CIS substrates are more randomly oriented than NREL sputtered ZnO onto NREL CIGS, for example (see Figure 8). The data were acquired for a CVD ZnO film grown by the baseline process onto Siemens CIS material. Three ZnO lines were observed, namely, the (110), (002) and (111) lines. Based on these results, the MOCVD films are more randomly oriented than sputtered films which are more strongly oriented along the (002) axis. Finally, the GIXRD study did not reveal any secondary phases in the ZnO buffer layer.

ZnO films have also been studied with ellipsometry. Two types of film were examined, those grown on CIS with the two-step, baseline process and films grown

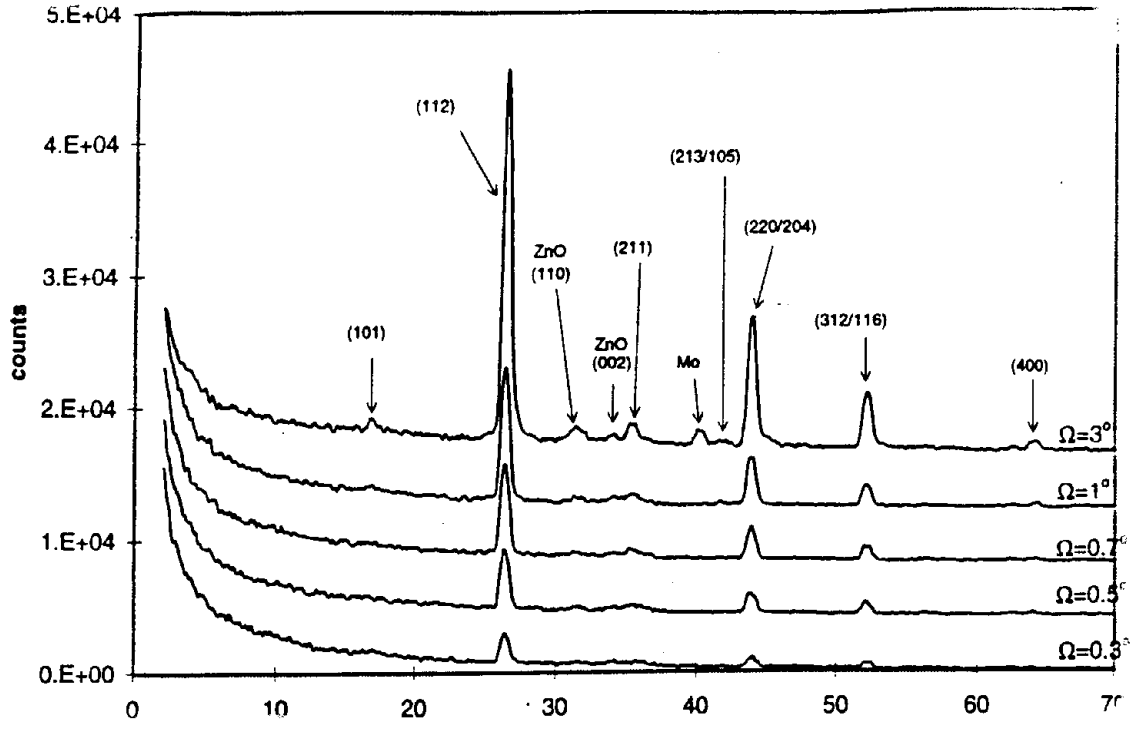

Figure 8. GIXRD data taken by NREL on a ZnO/CIS structure. The ZnO was grown by CVD and the CIS substrate was Siemens.

with a single step procedure at 100°C. One of the most significant conclusions to date is that the optical properties of films grown with two-step and single-step methods are essentially identical. Since solar cells based on a single step buffer layer are very poor, we tentatively conclude that the importance of the 250°C step in the growth process is not related to CIS film properties, but rather to ZnO/CIS interface properties. This conclusion is consistent with the hypothesis that the 250°C step results in a clean CIS surface.

2.4 Solar Cell Studies

ZnO/CIS solar cells have been fabricated by first depositing an i-ZnO buffer layer, followed by deposition of a low resistivity ZnO top contact layer and collector grid. Prior to growth of i-ZnO layers, substrates were subjected to a degreasing process consisting of rinses in TCA, acetone, methanol and DI water. Including the degreasing process is particularly important when substrates are mailed from one

location to another. To date we have relied on collaboration with Siemens, NREL and IEC for deposition of conductive ZnO. In some cases, the n-ZnO/i-ZnO/CIS structure was returned to WSU for collector grid and AR coating deposition. In other cases, the collector grid and AR coating were applied immediately after deposition of the n-ZnO.

Several completed cells have been fabricated with Siemens CIGSS substrates that had total area efficiencies in the 11 to 12 % range, and with Siemens CIS material that exhibited active area efficiencies of nearly 12 %. Cell efficiencies greater than 12 % were obtained with ZnO buffer layers combined with NREL CIGS substrates. Figure 9 shows I-V characteristics for a cell with a n-ZnO/i-ZnO/CIGS structure. The CIGS substrate was supplied to WSU by NREL for growth of an i-ZnO. After returning the i-ZnO/CIGS structure to NREL the cell was completed at NREL. Note that the total area efficiency was 12.7 %. Figure 10 gives illuminated and dark characteristics for another cell based on the i-ZnO/CIGS junction. The active area efficiency of 13.95 % is one of the best results, if not the best, for a 'direct ZnO' cell. In this case, after the i-ZnO layer was grown by WSU on an NREL CIGS substrate, i-ZnO/CIGS structures were sent to IEC for TCO deposition, contacting and testing. After depositing conductive n-ZnO films with a sheet resistance of 15 ohms/sq., devices were formed that were 0.3 x 0.5 cm. Ni strips were then placed on the devices leaving active areas of 0.13 cm^2. Illuminated characteristics of devices were measured at 30 °C with an ORIEL simulator and at a level of 100 mW/cm^2. External quantum efficiencies for ZnO/CIGS and ZnO/CIS cells are plotted vs wavelength in Figure 11. The abrupt rise at 400 nm is characteristic of ZnO buffer layers. Some of the best cell results achieved with WSU i-ZnO buffer layers are tabulated in Table 1.

Cells with CdS buffer layers were also processed at NREL with CIGS material from the same plate as that used for the 13.9 % direct ZnO cell. The two best total area efficiencies achieved with the CdS/CIGS structures were 14.5 and 15.3 %. Thus, the i-ZnO/CIGS cells exhibited properties nearly as good as the NREL CdS/CIGS cells.

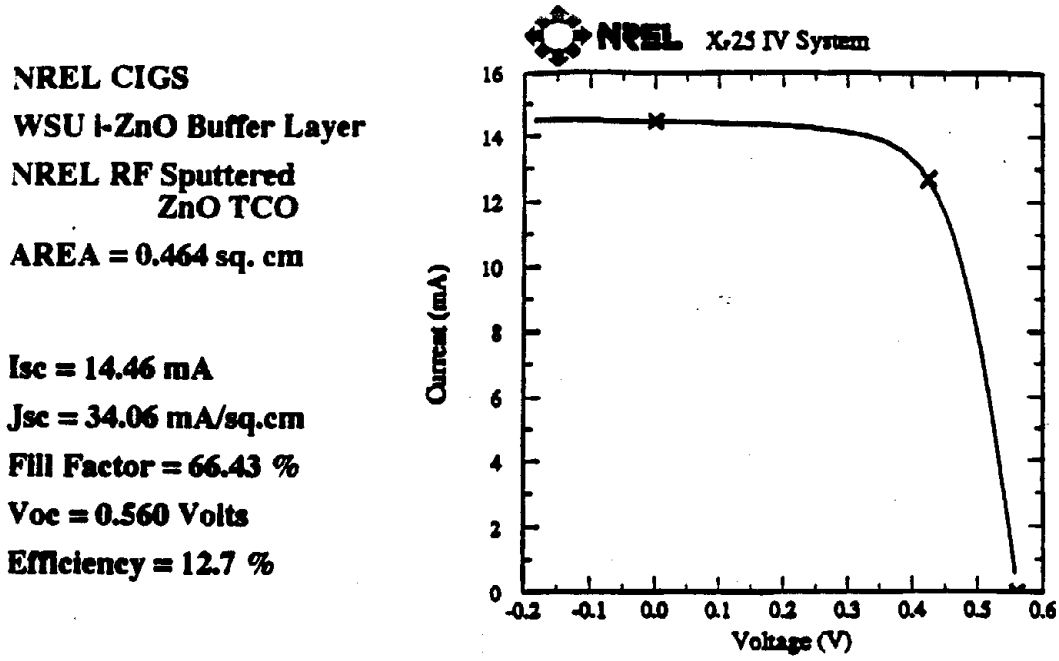

Figure 9. Total area I-V characteristics of a n-ZnO/i-ZnO/CIGS cell fabricated through a collaborative effort between WSU and NREL.

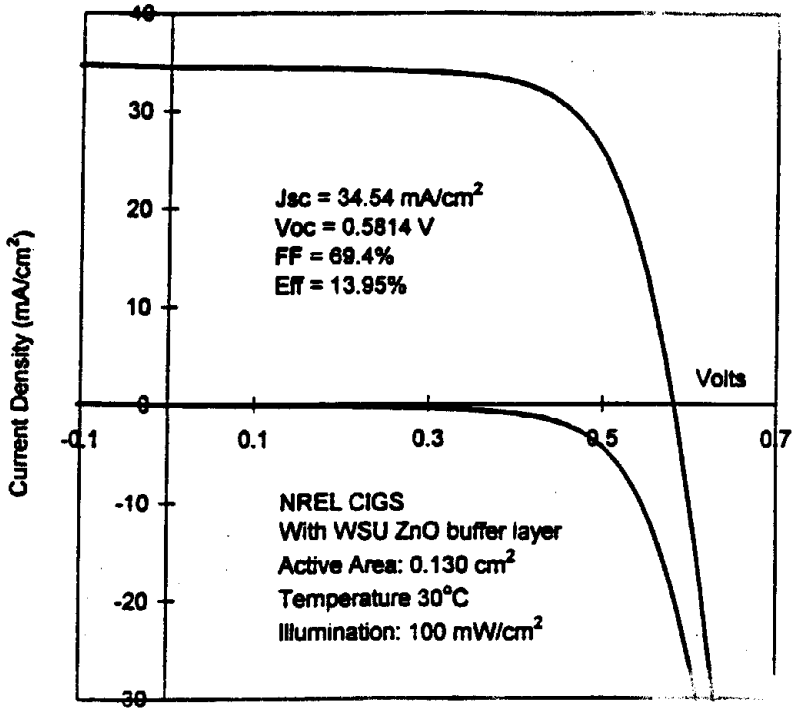

Figure 10. Active area I-V characteristics for a n-ZnO/i-ZnO/CIGS cell structure.

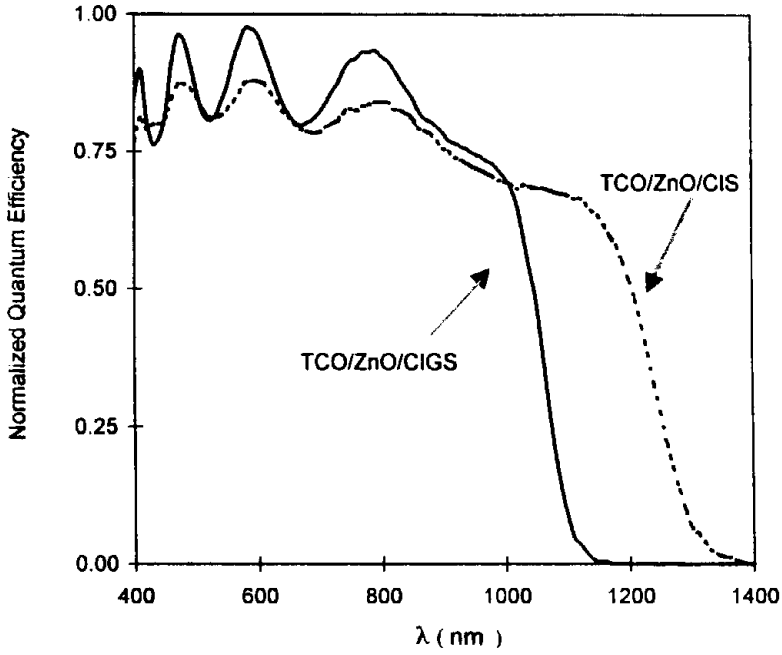

Figure 11. Normalized quantum efficiency curves for i-ZnO/CIGS cells formed on NREL CIGS and Siemens CIS .

TABLE 1. Cell Results

	Buffer Layer	Jsc (mA/cm2)	Voc (mV)	FF (%)	Efficiency (%)
NREL SUBSTRATES					
NREL C679-9 [2]	CVD ZnO	33.5	524	69.5	12.2
NREL M1455-1#1 [1]	CVD ZnO	34.06	560	66.4	12.7
NREL C679-5 [2]	CVD ZnO	34.5	581	69.2	13.9
SIEMENS SUBSTRATES					
SSI 97XC019 [2]	CVD ZnO	40.7	439	66.9	12.0
SSI 97XC021 [2]	CVD ZnO	36.4	455	71.0	11.7
SSI 97XC016 [2]	CVD ZnO	37.5	437	69.6	11.4

1. Measurements made at NREL at 25°C and are total area values.
2. Measurements made at IEC at 30°C and are active area values.

3. ZnSe BUFFER LAYER STUDIES

Although our focus has been mainly on ZnO buffer layers over the last two years, work was also carried out on ZnSe buffer layers. The approach to investigating ZnSe films was similar to that described for ZnO. Experimental studies were carried out with CIS and CIGSS substrates provided by Siemens Solar. ZnSe films were deposited by a CVD process which involved the reaction of a zinc adduct and H_2Se. Using Al/ZnSe/CIS test cells for process development, the optimum thickness for a ZnSe buffer layer was determined in a previous program to be in the range of 150Å to 200Å for Siemens CIS material, and between 80Å and 120Å for the graded absorber material (CIGSS). If ZnSe buffer layers exceeded these values significantly, the short-circuit current would be reduced to zero. This effect is consistent with results reported in the literature indicating that there is a 0.9 eV band offset at the ZnSe-CIS interface when semi-infinite slabs of ZnSe and CIS are in contact. Our studies suggest that the conduction band offset is not fully established for thin films. However, test cell studies have indicated that high efficiency ZnSe/CIS and ZnSe/CIGS cells can be fabricated. For example, consider the dark and illuminated characteristics shown in Figure 12 for a test cell formed on NREL CIGS material. The test cell structure was similar to that described in Figure 1 with ZnSe replacing ZnO. The short circuit current was set to a value expected for the NREL material.

Completed cells were fabricated by utilizing a low resistance ZnO top contact layer deposited by Siemens or by NREL, and then depositing an Al/Ag collector grid at WSU. The best efficiency achieved for a ZnSe/CIS cell was a total area value of 9.5 %. Illuminated I-V characteristics of this cell are given in Figure 13. This cell was the first ZnSe/CIS device that did not exhibit extreme degradation of properties as a result of the TCO deposition process. The conductive ZnO layer for this cell was deposited by RF sputtering at NREL. Deposition of n-ZnO onto ZnSe/CIS structures by a CVD process at Siemens always resulted in a cell with very poor properties. Results for the cell described in Figure 13 are encouraging. Further optimization of TCO deposition process for ZnSe/CIS structures is required.

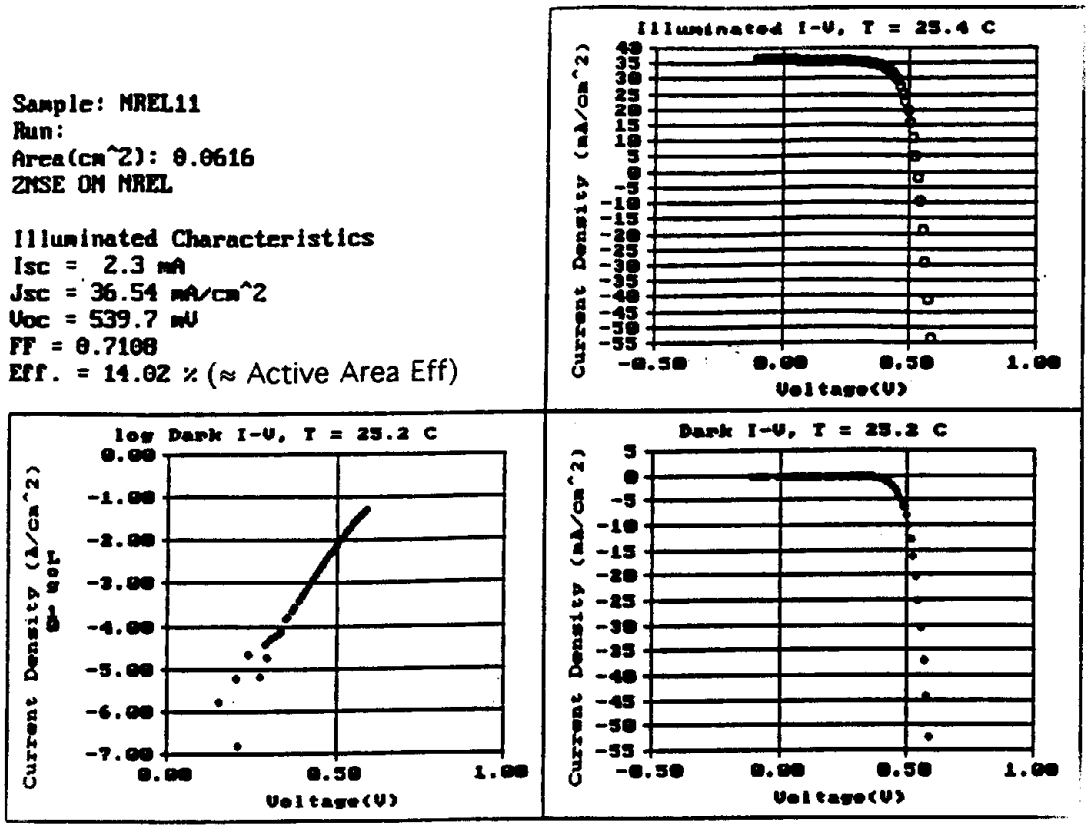

Figure 12. ZnSe/CIGS test cell I-V characteristics. The CIGS was NREL material and the ZnSe film was deposited by CVD at WSU.

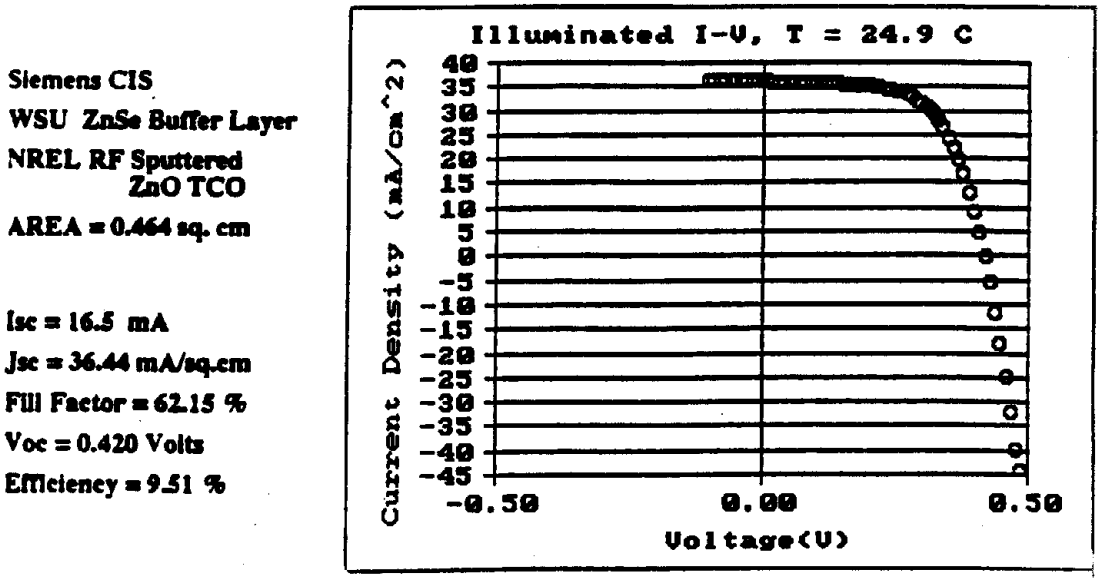

Figure 13. Illuminated I-V characteristics measured by WSU for a completed ZnSe/CIS solar cell.

4. In_xSe_y BUFFER LAYER STUDIES

Investigation of InSe buffer layers was also initiated this past year. InSe films were grown by reacting H_2Se and ethyldimethylindium with substrate temperatures in the range of 300 to 400 °C. Test cell studies have shown promise. Raman spectroscopic analyses indicate that the crystallinity of InSe films improve as T_{sub} is increased from 300°C to 400°C. Films grown near 300°C appear to be amorphous. The Raman studies also suggest that the amount of the γ -In_2Se_3 phase increases with T_{sub}. This phase has a bandgap of approximately 2.0 eV.

InSe buffer layers were investigated by characterizing test cells formed on Siemens CIS and CIGSS substrates. Each run also included film growth on glass and silicon substrates. Most of the work to date has involved growth at 300°C. It appears that with no film growth occurs at 250 °C, whereas growth does definitely occur in the 300°C to 450°C range. Results for test cells fabricated by depositing Al onto InSe/CIS structures are tabulated in Table 1. Some encouraging results have been obtained. In particular, Test Cell 96NC007 (Siemens CIS material) exhibited an open circuit voltage of 420 mV, a fill-factor of 0.67 and an efficiency of 11.4 % when the Jsc-value was set to 40 mA/cm^2. The performance of this test cell is comparable to the best results obtained with ZnO buffers on CIS, but not as good as test cells fabricated with ZnSe buffer layers. * Only two devices based on Siemens CIGSS material were studied. As in the case of CIS material, results are promising.

TABLE 1 -- Test Cell Results For InSe/CIS Structures

Samples	Run	Substrate	EDMIn	H2Se	VI/III	Growth	Test Cells*			
(Relatives)		Temperature	(sccm)	(sccm)	Ratio	Time	Jsc	Voc	FF	Eff
		(℃)	(μmol/min)	(μmol/min)	(μmol/μmol)	(sec)	(mA/cm^2)	(mV)		(%)
Siemens CIS										
96NC006	A60408	250	10	400	709	1040	40	230	0.534	4.82
(CIS)			0.23	163						
96NC007	A60410	300	10	400	709	304	40	420	0.67	11.4
(CIS)			0.23	163						
96NC008	B60410	300	80	400	88.6	800	40	383	0.571	7.67
(CIS)			1.84	163						
96NC010	A60509	300	40	400	177	300	40	382	0.578	8.82
(CIS)			0.92	163						
96NC 12	B60509	300	10	400	709	650	40	417	0.64	10.8
(CIS)			0.23	163						
Siemens CIGSS (Graded Absorber)										
96NC009	A60509	300	40	400	177	300	40	463	0.595	11.3
(CIGSS)			0.92	163						
96NC011	B60509	300	10	400	709	650	40	458	0.528	9.65
(CIGSS)			0.23	163						
*	(1) Test Cell Illuminated I-V Measured With ELH Lamps And Jsc = 40 mA/cm^2.									
	(2) EDMIn μmol/min = 0.173 x #sccm									
	(3) H2Se μmol/min = 0.409 x #sccm									

5. SIMULATION STUDIES

Simulation studies using PC-1D indicate that a resistive buffer layer combined with a CIS substrate should yield a higher efficiency compared to a structure with a low resistivity buffer layer -- or with the TCO in direct contact with CIS. This prediction is in general agreement with experimental results. In particular, one predicts that a ZnO/CIS cell with the ZnO layer having a resistivity of 0.01 ohm-cm should produce power with an efficiency of 8 % , whereas 11 % should be obtained with a ZnO buffer layer characterized by a resistivity of 1E4 ohm-cm. These calculations assume the excess carrier lifetime is 40 psec within the CIS material. Experimentally. one finds cell efficiencies are typically 4 % when a conductive ZnO is in direct contact with CIS. Additional studies were carried out in an effort to understand the cause of this discrepancy.

Modeling calculations were conducted to examine the effects of interface recombination velocity and excess carrier lifetime. Figures 14 and 15 describe results of these studies. The solid lines describe results of simulations and the data points refer experimental results for test cells made with ZnO buffer layers having a range of as-deposited resistivities. Figure 14 clearly indicates that we can not explain experimental results by simply assuming the deposition of low resistivity ZnO onto CIS leads to a high value for the interface recombination velocity. Referring to Figure 15, we conclude that one possible explanation of the low efficiencies for in the case of low buffer layer resistivities is that the deposition process results in reduced values of excess carrier lifetimes -- that is, increased densities of recombination centers. In our case, the low resistivity ZnO is grown by using a relatively high flow of Zn when growing ZnO. Thus, the presence of excess zinc may result in an increased density of recombination sites. Deposition of low resistivity ZnO usually involves the incorporation of dopants, which may also provide recombination sites. In conclusion, we postulate that a possible explanation of the apparent requirement for a high resistivity buffer layer for CIS-

based cells is that deposition of low resistivity films directly on CIS and related alloys leads to enhanced recombination within the CIS material.

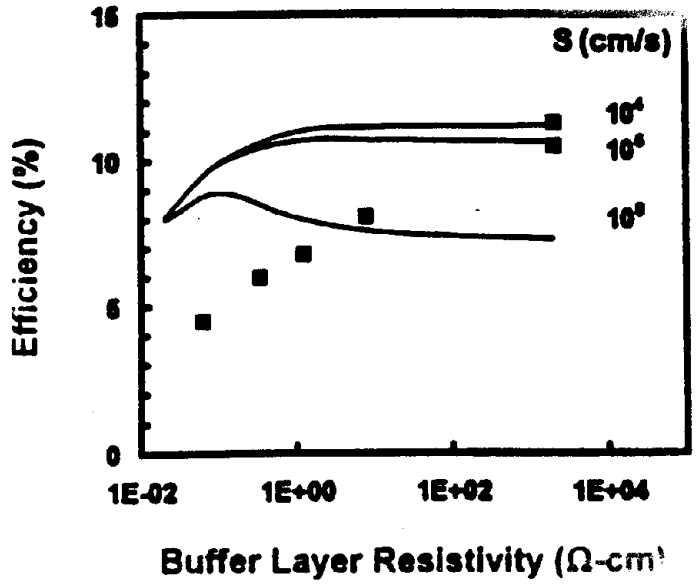

Figure 14. Calculated efficiency vs ZnO buffer layer resistivity for a CIS cell with varied values of surface recombination velocity and a ZnO buffer layer thickness of 300 Å. The data points are experimental results for test cells with CVD ZnO buffer layers.

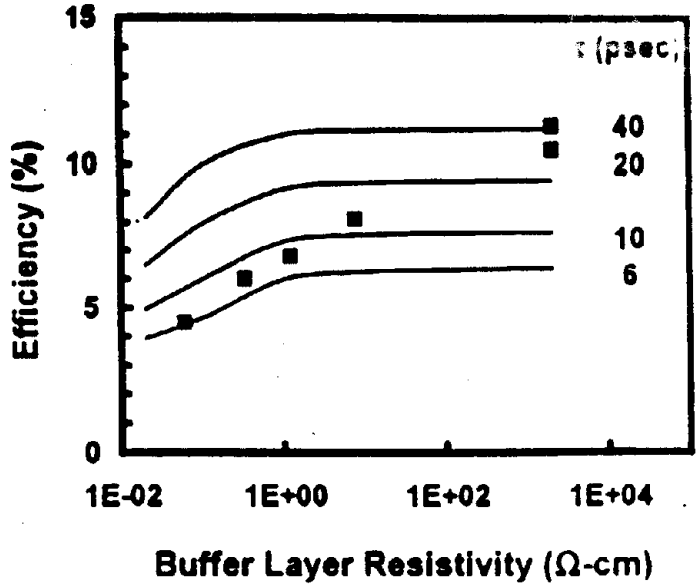

Figure 15 Calculated efficiency vs ZnO buffer layer resistivity for a CIS cell with varied values of excess carrier lifetime and a ZnO buffer layer thickness of 300 Å and S =1E4 cm/s. The data points are experimental results for test cells with CVD ZnO buffer layers.

6. CONCLUSIONS

This work has resulted in the demonstration of high efficiency CIGS cells based on highly resistive ZnO buffer layers grown by MOCVD. One cell based on NREL CIGS and a ZnO buffer layer exhibited an active area efficiency of nearly 14 %. This result is one of the best efficiencies reported for a "direct" ZnO/CIGS cell made with a vacuum process. This work has established that the buffer layer is truly ZnO, and not an alloy resulting from interdiffusion of ZnO and CIGS. It has also been established that two step growth procedures like that described as 'baseline' and 'modified' lead to efficient cells. In order to achieve high efficiencies, it is necessary for ZnO buffer layers to have resistivities greater than 10^4 ohm-cm. Efficient cells are obtained whether the high resistivity is achieved as-grown, or after exposure to air. Since cell efficiencies are lower than predicted by simulation studies when the buffer resistivity is lower than 10^4 ohm-cm, we conclude that the resistivity requirement is simply related to processing. In particular, the resistivity correlates with the excess zinc in the MOCVD ZnO film, which can in turn diffuse into the CIS absorber and possibly cause enhanced current loss mechanisms. It is also possible that the benefits of the resistive buffer layer result from mechanisms that are not included in the PC-1D model. Future studies will focus on identifying process pathways that will lead to resistive ZnO buffer layers, and thus large cell efficiencies.

A limited effort was devoted to ZnSe buffer layers. A completed cell with a ZnSe buffer layer and RF sputtered ZnO TCO was fabricated and produced power with a total area efficiency of 9.5 %. Future studies will concentrate on the development of approaches to deposit conductive ZnO on top of the ZnSe buffer layer without degrading properties of the ZnSe/CIS structure.

ACKNOWLEDGMENTS

We wish to thank Bolko von Roedern of NREL for his guidance as our contract monitor, Kannan Ramanathan and Miguel Contreras of NREL for providing substrates and other technical support, Siemens Solar for providing substrates and William Shafarman for his technical support at IEC.

REFERENCES

1. L.C. Olsen," Investigation Of Polycrystalline Thin-Film $CuInSe_2$ Solar Cells Based on ZnSe and ZnO Buffer Layers," NREL/TP-451-21406, June, 1996.

2. D. Tarrant and J. Ermer, "I-III-VI2 Multinary Solar Cells Based On $CuInSe_2$," Twenty Third IEEE PVSC, 1993, pp. 372 - 378.

3. Miguel A. Contreras, et al., "High Efficiency $Cu(In,Ga)Se_2$-Based Solar Cells," First WCPEC, 1994, pp. 68 - 75.

4. J. Kessler, et al., "Interface Engineering Between CuInSe2 and ZnO," Twenty Third IEEE PVSC, 1993, pp. 447-452.

5. William N. Shafarman, et al., "Device And Material Characterization Of $Cu(In,Ga)Se_2$ Solar Cells With Increasing Bandgap," J. Appl. Phys. 79 (9), 1 May 1996.

REPORT DOCUMENTATION PAGE

Form Approved
OMB NO. 0704-0188

Public reporting burden for this collection of information is estimated to average 1 hour per response, including the time for reviewing instructions, searching existing data sources, gathering and maintaining the data needed, and completing and reviewing the collection of information. Send comments regarding this burden estimate or any other aspect of this collection of information, including suggestions for reducing this burden, to Washington Headquarters Services, Directorate for Information Operations and Reports, 1215 Jefferson Davis Highway, Suite 1204, Arlington, VA 22202-4302, and to the Office of Management and Budget, Paperwork Reduction Project (0704-0188), Washington, DC 20503.

1. AGENCY USE ONLY (Leave blank)	2. REPORT DATE	3. REPORT TYPE AND DATES COVERED
	October 1998	Final Report; 3 November 1995–31 December 1997

4. TITLE AND SUBTITLE
Alternative Window Schemes for $CuInSe_2$-Based Solar Cells; Final Report, 3 November 1995–31 December 1997

5. FUNDING NUMBERS
C: XAF-6-15375-01
TA: PV804401

6. AUTHOR(S)
L.C. Olsen

7. PERFORMING ORGANIZATION NAME(S) AND ADDRESS(ES)
Electronic Materials Laboratory
Washington State University at Tri-Cities
Richland, Washington

8. PERFORMING ORGANIZATION REPORT NUMBER

9. SPONSORING/MONITORING AGENCY NAME(S) AND ADDRESS(ES)
National Renewable Energy Laboratory
1617 Cole Blvd.
Golden, CO 80401-3393

10. SPONSORING/MONITORING AGENCY REPORT NUMBER
SR-520-25613

11. SUPPLEMENTARY NOTES
NREL Technical Monitor: B. von Roedern

12a. DISTRIBUTION/AVAILABILITY STATEMENT
National Technical Information Service
U.S. Department of Commerce
5285 Port Royal Road
Springfield, VA 22161

12b. DISTRIBUTION CODE

13. ABSTRACT *(Maximum 200 words)*

This work demonstrated high-efficiency CIGS cells based on highly resistive ZnO buffer layers grown by MOCVD. One cell based on NREL CIGS and a ZnO buffer layer exhibited an active-area efficiency of nearly 14%. This result is one of the best efficiencies reported for a "direct" ZnO/CIGS cell made with a vacuum process. This work has established that the buffer layer is truly ZnO and not an alloy resulting from interdiffusion of ZnO and CIGS. Also established is that a two-step growth procedure like those described as "baseline" and "modified" lead to efficient cells. To achieve high efficiencies, ZnO buffer layers must have resistivities greater than 10^4 ohm-cm. Efficient cells are obtained whether the high resistivity is achieved as-grown, or after exposure to air. Because cell efficiencies are lower than predicted by simulation studies when the buffer resistivity is lower than 10^4ohm-cm, we conclude that the resistivity is simply related to processing. In particular, the resistivity correlates with the excess zinc in the MOCVD ZnO film, which can, in turn, diffuse into the CIS absorber and possibly cause enhanced current loss mechanisms. Future studies will focus on identifying process pathways that will lead to resistive ZnO buffer layers, and thus, large cell efficiencies. A limited effort was devoted to ZnSe buffer layers. A completed cell with a ZnSe buffer layer and RF-sputtered ZnO TCO was fabricated and produced power with a total-area efficiency of 9.5%. Future studies will concentrate on developing approaches to deposit conductive ZnO on top of the ZnSe buffer layer without degrading properties of the ZnSe/CIS structure.

14. SUBJECT TERMS
photovoltaics ; copper indium diselenide ; alternative window layers ; solar cells ; buffer layers ; zinc oxide ; zinc selenide

15. NUMBER OF PAGES
29

16. PRICE CODE

17. SECURITY CLASSIFICATION OF REPORT	18. SECURITY CLASSIFICATION OF THIS PAGE	19. SECURITY CLASSIFICATION OF ABSTRACT	20. LIMITATION OF ABSTRACT
Unclassified	Unclassified	Unclassified	UL